J Mater Sci

Electrical enhancement of radiation-vulcanized natural rubber latex added with reduced graphene oxide additives for supercapacitor electrodes

A. B. Suriani[1,2,*], M. D. Nurhafizah[1,2], A. Mohamed[1,3], A. K. Masrom[4], M. H. Mamat[5], M. F. Malek[5,6], M. K. Ahmad[7], M. S. Rosmi[3,8], and M. Tanemura[8]

[1] Nanotechnology Research Center, Faculty of Science and Mathematics, Universiti Pendidikan Sultan Idris, 35900 Tanjung Malim, Perak, Malaysia
[2] Department of Physics, Faculty of Science and Mathematics, Universiti Pendidikan Sultan Idris, 35900 Tanjung Malim, Perak, Malaysia
[3] Department of Chemistry, Faculty of Science and Mathematics, Universiti Pendidikan Sultan Idris, 35900 Tanjung Malim, Perak, Malaysia
[4] National Nanotechnology Center (NNC), Ministry of Science, Technology and Innovation, Technology Park Malaysia, 57000 Kuala Lumpur, Malaysia
[5] NANO-ElecTronic Centre (NET), Faculty of Electrical Engineering, Universiti Teknologi MARA (UiTM), 40450 Shah Alam, Selangor, Malaysia
[6] NANO-SciTech Centre (NST), Institute of Science (IOS), Universiti Teknologi MARA (UiTM), 40450 Shah Alam, Selangor, Malaysia
[7] Microelectronic and Nanotechnology-Shamsuddin Research Centre (MiNT-SRC), Faculty of Electrical and Electronic Engineering, Universiti Tun Hussein Onn Malaysia, 86400 Parit Raja, Batu Pahat, Johor, Malaysia
[8] Department of Frontier Materials, Nagoya Institute of Technology, Gokiso-cho, Showa-ku, Nagoya 466-8555, Japan

Received: 17 December 2016
Accepted: 6 February 2017

ABSTRACT

An insulating polymer, radiation vulcanization natural of rubber latex (RVNRL), was successfully converted into electrically conductive nanocomposite by the addition of reduced graphene oxide (rGO) assisted by sodium 1,4-bis(neopentyloxy)-3-(neopentyloxycarbonyl)-1,4-dioxobutane-2-sulfonate (TC14) surfactant. The starting material, graphene oxide (GO), was initially synthesized by electrochemical exfoliation assisted by TC14 surfactant. Then, GO/RVNRL nanocomposite was fabricated by latex technology. For rGO/RVNRL nanocomposite, the synthesized GO was further reduced to rGO using hydrazine hydrate and showed electrical enhancement up to 1.32×10^{-3} S cm^{-1} compared with GO when composited with RVNRL (8.64×10^{-4} S cm^{-1}). For comparison, rGO/RVNRL nanocomposite assisted by the commercially available surfactant sodium dodecyl sulfate was prepared, and its electrical conductivity was found to be 1.79×10^{-5} S cm^{-1}, which was several orders of magnitude lower than those of

Address correspondence to E-mail: absuriani@yahoo.com

DOI 10.1007/s10853-017-0897-9

Published online: 16 February 2017

GO/RVNRL and rGO/RVNRL nanocomposites prepared with TC14 surfactant. C–V measurements taken for TC14-rGO/RVNRL and TC14-GO/RVNRL nanocomposites showed specific capacitances of 95 and 63 F g^{-1}, respectively. The structural properties of nanocomposites were characterized using FESEM, HR-TEM, UV–Vis, micro-Raman, XRD, FT-IR spectroscopy, and TGA studies. This study was the first to report on the success of converting the insulator polymer RVNRL into a conductive nanocomposite assisted by TC14 surfactant. The nanocomposite can be a new electrode material for supercapacitor application.

Introduction

The natural rubber industry has grown steadily since the 1960s; consumption of natural rubber has increased because of massive demand for various applications, such as in aerospace, defense industry, biomedicine, and electronics [1–3]. Liquid natural rubber latex (NRL) is preferred because it is easily processable and cheap and contains abundant raw materials for fabrication and modification of nanocomposites. NRL can be categorized into two groups: (1) pure NRL (collected from rubber trees and only ammonia was used for durable purpose) and (2) synthetic NRL (processed and blended with other activators, antioxidants, and cross-linking agents). Pure NRL is weak for practical uses without being chemically cross-linked because it is sticky and sensitive to heat and has low solvent resistance and non-elastic properties [4]. Thus far, sulfur vulcanization (SV) and radiation vulcanization (RV) are more popular than other methods for NRL vulcanization. In the recent years, two types of vulcanization using RV method are commonly used for rubber cross-linking and are preferred than SV method; these types of vulcanization include radiation through high penetration of gamma ray from a radioactive source (i.e., ^{60}Co) and acceleration of low-energy electron beams from the electron accelerator [4]. Currently, selection of radiation-vulcanized natural rubber latex (RVNRL) is favorable in rubber industries, especially for the production of condoms and gloves [2, 5]; RVNRL exhibits low cytotoxicity and highly degradable nature as well as lower emission of sulfur dioxide than sulfur-vulcanized natural rubber latex (SVNRL) [4]. The synthetic rubber RVNRL, which is used for non-sulfur vulcanization or zinc-free vulcanizing system, possesses high thermal stability and modulus strength against resistance [6]. Since the 1950s, various works have been systematically conducted on RVNRL because it satisfies high levels of end-product applications over SVNRL [7].

NRL polymers exhibit multifunctional properties, such as mechanical, thermal, gas barrier, and electrical conductivity [8–10]. NRL polymers also suffer from brittle fracture and poor crack growth resistance [10, 11]. This limitation could be resolved by adding nanofillers. Nanofillers exist at least in the one-dimensional (1D) range to enhance nanocomposite performance. Previous studies showed that silica, mica (1D) [12, 13], carbon black, and carbon nanotubes (2D) [14, 15] are effective nanofillers for elastomer nanocomposites. High conductive nanofillers are crucial to improve the properties of NRL and its derivative groups because of the low conductivity of the nanocomposites. In addition, the distribution of the high surface area of nanofillers can affect the properties of nanocomposites produced [9]. Graphene (GE) structures feature abnormal electrical properties and high surface area [16, 17]; hence, this extraordinary carbon material has been extensively investigated in many fields, particularly in polymer nanocomposites, since its discovery in 2004 [18, 19]. The filled NRL matrix with GE dispersion confers NRL with outstanding properties. However, only few studies have been documented on GE-filled rubber nanocomposites because of (1) lack of functional groups in GE that efficiently interact with the NRL matrix, (2) high surface area, which tends to agglomerate in nanocomposites and even in the earlier preparations in a water-based medium, and (3) high manufacturing cost. Therefore, fabrication of graphene oxide (GO)/NRL or reduced graphene oxide (rGO)/NRL polymer nanocomposites has been extensively studied [20].

GO is a well-known multilayer planar sheet that is oxidized from graphite sources through various top-to-bottom approaches. rGO consists of several layers

of graphite, which has been reduced from the GO sheets through two processes: (1) chemical reduction, such as that performed with hydrazine hydrate [21], and (2) thermal treatment, such as that performed through microwave irradiation [22]. The rGO is highly valuable due to the restoration of π-conjugated system and the presence of reactive sites along the structures renders it soluble in water-based polymers [23]. Recently, the treatment of GO solution using hydrazine hydrate has gained interest due to several benefits such as reduction procedures that can be operated at a low temperature and low consumption of a certain volume of GO solution to produce a bulk quantity of rGO in a short time [24]. Recently, the introduction of chemically produced rGO materials gives highest efficiency in the energy storage and nanoelectronic applications due to efficient interaction between the oxygen containing functional groups with the electrolyte [25, 26]. Previously, Jin et al. [25] have adopted rGO instead of GO materials for the use as electrode materials of supercapacitor. Therefore, instead of using GO, the widely used rGO in the nanocomposite has clearly shown an interesting increment of capacitive behavior in the electrochemical supercapacitor due to outstanding properties contained in the graphene structure.

Numerous studies investigated the synergetic effects of various polymers with GO and rGO materials. Elastomer nanocomposites can be produced through three main processing methods: melt compounding [27], solution mixing [28], and in situ polymerization [29]. Our previous studies demonstrated the effective dispersing role of the tailgroup surfactant, and the use of tripletail sodium 1,4-bis(-neopentyloxy)-3-(neopentyloxycarbonyl)-1,4-dioxobutane-2-sulfonate (TC14) surfactant above the critical micelle concentration (cmc) (21.63 mM) has proven to increase the dispersion level between the GO and NRL matrix. This is despite the fact that GO is far more difficult to disperse due to strong van der Waals interactions [30–32]. The proposed graphene suspension mechanism by TC14 relies on the low surface tension of tripletail TC14 that gives triple interaction to hydrophobic carbonaceous materials. Therefore, we extended our work and investigated the effectiveness of the TC14 surfactant toward the new system of rGO dispersions in the RVNRL matrix because of the similarity of elastomer groups to NRL polymer. To the best of our knowledge, this work is the first attempt to prepare electrically conductive RVNRL polymer-based nanocomposite by introducing rGO dispersions assisted by TC14 surfactant, which is believed to serve as versatile nanocomposite electrodes for supercapacitor application.

Materials and methods

Two pieces of high-purity graphite rods (99.99%) with the diameter and length of 10 and 150 mm, respectively, were purchased from Good Fellow Company, Germany. RVNRL was collected from Malaysian Institute of Nuclear Technology Research, Bangi, Malaysia. The RVNRL polymer (52% of TSC) was irradiated with doses up to 12 kGy using γ-rays from a ^{60}Co source at a constant dose rate (2 kGy/h) for 6 h of radiation time.

Preparation of rGO/NRL nanocomposite through two-step method

Hydrazine hydrate (Merck; 80% solution in water) was consumed as a reducing agent for rGO solution. The 1:100 volume ratio of hydrazine hydrate to GO solution was mixed in a triple neck, round-bottom flask that was readily immersed in a hot water. The mixture was stirred for 24 h using a magnetic stirrer, and the temperature was maintained around ~95 °C. Then, the dispersions were subjected to ultrasonic dissolution for 30 min. The fabrication process of 1:1 volume ratio rGO/NRL nanocomposite was conducted by similar stirring and ultrasonication processes as in a previous study [30, 33]. In addition, for comparison purposes, the rGO/RVNRL nanocomposite assisted by the commercially available surfactant sodium dodecyl sulfate (SDS) was prepared with similar fabrication procedures, in which a 0.1 M SDS electrolyte solution was used with an applied voltage of 7 V at 24 h to synthesize GO. The dispersion was then stirred (3000 rpm) and sonicated for 2 h with the introduction of RVNRL matrix before overnight cast drying. A total of ~4.15–4.30 wt% of GO and rGO was consumed during the fabrication of the nanocomposites assisted by TC14 and SDS surfactants.

Characterizations

The electrical properties of the nanocomposites were measured using a standard four-point probe instrument (Keithley 2636A). Surface morphologies of the

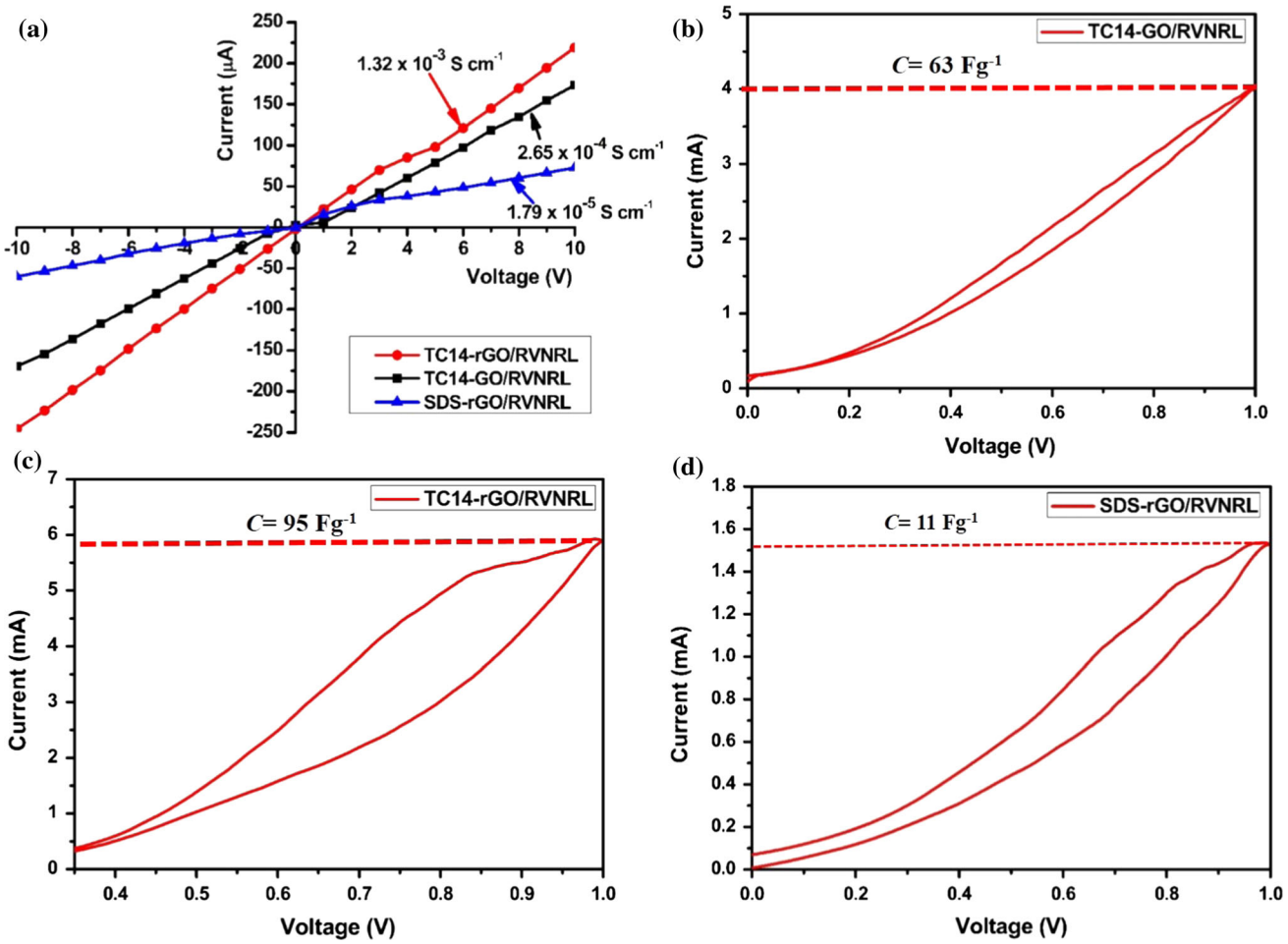

Figure 1 I–V and C–V curves of nanocomposite.

pristine GO and rGO were conducted using HRTEM (JEOL JEM 2100) at 160 kV of accelerating voltage. Meanwhile, the cryogenically nanocomposite samples using Leica Ultramicrotome, UC6, at room temperature with a diamond knife at temperature −110 °C were used. The nanocomposite samples were then analyzed using FESEM (Hitachi SU8020) with an operating voltage at 2–5 kV. Further analysis of the reduction process from GO to rGO was confirmed with an Agilent Cary 60 spectrophotometer, and the absorption spectrum was recorded within 200–800 nm. For capacitance measurement, the cyclic voltammetry measurement (GamryPotentiostat Series-G750 USA) was used for electrochemical testing. Crystallinity was measured using micro-Raman spectroscopy (RenishawInVia Raman Microscope) with 514 nm wavelength using Ar^+ ion laser recorded from 400 to 4000 cm^{-1}, and XRD patterns were collected between 0° and 40° from a diffractometer of PANalytical X'pert Pro monochromatized CuKα ($\lambda = 1.54$ Å). FT-IR was carried out using a Thermo scientific Nicolet 6700 spectrophotometer within 4000–500 cm^{-1} to confirm the interfacial interaction between the rGO dispersions and the RVNRL matrix. Meanwhile, the thermal stability of the nanocomposite samples was studied using a thermogravimetric analysis (TGA) Mettler Toledo SDTA 851 at a heating rate of 10 °C min^{-1} under nitrogen atmosphere.

Results and discussion

After the reduction process, the conductivity of the TC14-rGO/RVNRL nanocomposite obtained was found to be 1.32×10^{-3} S cm^{-1}, which was higher than the TC14-GO/RVNRL nanocomposite (2.65×10^{-4} S cm^{-1}). The results obtained were also found much higher than the nanocomposite assisted by

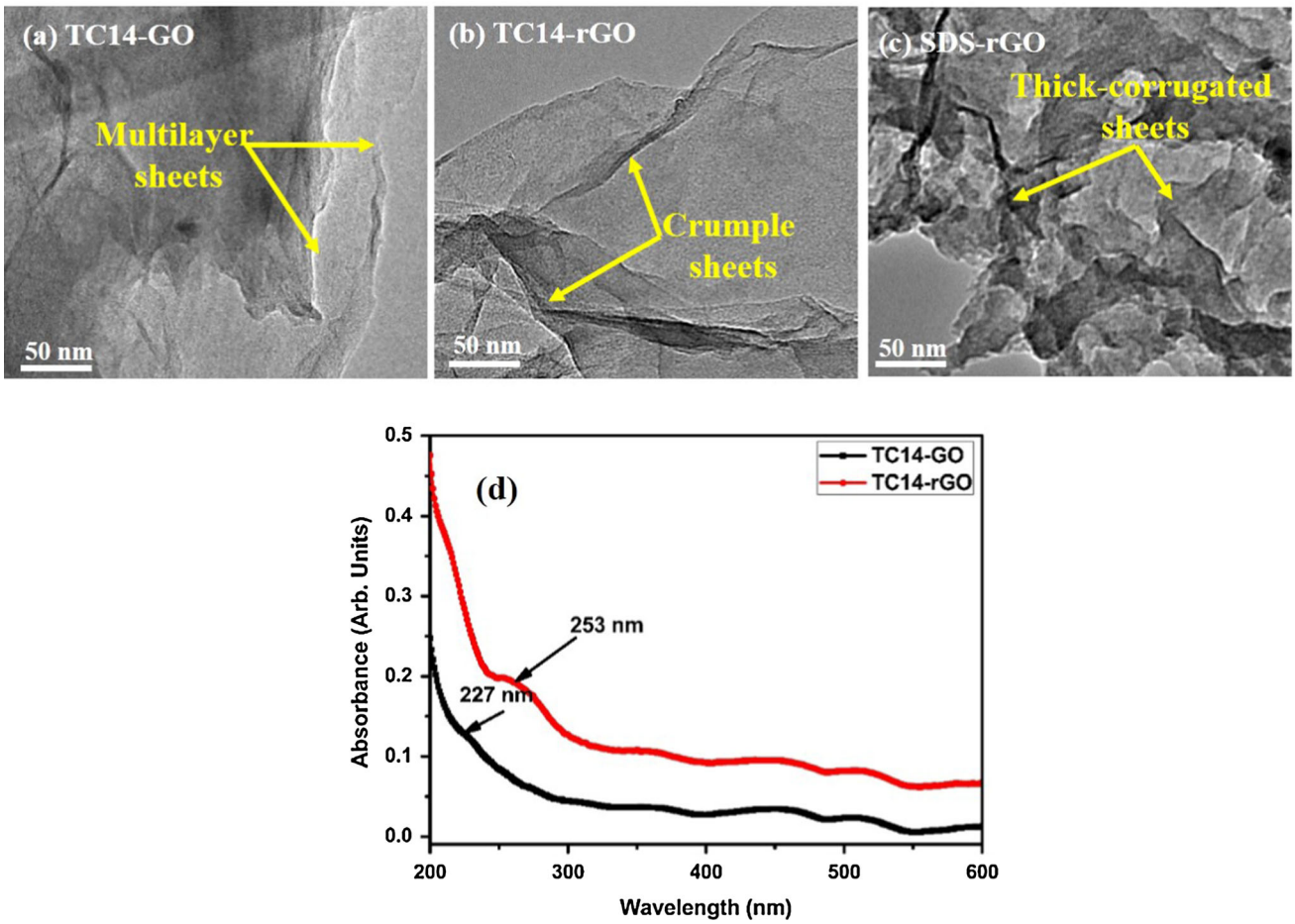

Figure 2 HRTEM of GO- and rGO-assisted surfactants.

commercially available SDS surfactant (1.79×10^{-5} S cm^{-1}) (Fig. 1a). This finding shows that the introduction of rGO sheets assisted by low surface tension of tripletail TC14 surfactant above its cmc level in the RVNRL matrix led to effective adsorption onto the rGO sheets and can easily form a high conductive nanocomposite as compared with the SDS surfactant [30–32, 34]. In fact, the value of electrical conductivity for nanocomposite assisted by SDS surfactant was much lower than the nanocomposite assisted by TC14 surfactant for both GO and rGO sheets.

C–V measurement was taken to determine the ability of highly conductive and homogenous rGO/RVNRL and GO/RVNRL nanocomposite-assisted surfactants. Higher capacitance value of 95 F g^{-1} at 100 scan rates was measured for TC14-rGO/RVNRL as compared with the TC14-GO/RVNRL nanocomposite with lower capacitance value of 63 F g^{-1} (Fig. 1b–c). This finding represented the electrocatalytic activity of rGO on the surface of electrodes [35]. The incorporation of RVNRL polymer actually contributed to the slightly increased charge-transfer resistance in the rGO/RVNRL nanocomposite [36]. Nonetheless, the wrinkled structures of the produced rGO offered better electrolyte ion accessibility, which not only penetrated the outer region of rGO but also its inner region, compared with the highly agglomerated structures of GO sheets. This phenomenon aided the enhancement of capacitance performance [37]. In addition, the wettability of rGO/RVNRL nanocomposite electrodes was also enhanced by the residual functional groups on the rGO sheets, which increased the number of hydrophobic polar sites and thus contributed to the capacitance measured [38, 39]. The present study open a new pathway to producing simple, green, and low-cost electrode materials for fast charge–discharge supercapacitor application. These results confirmed the conversion of insulating RVNRL matrix to highly conductive nanocomposite was induced by the introduction of TC14-assisted

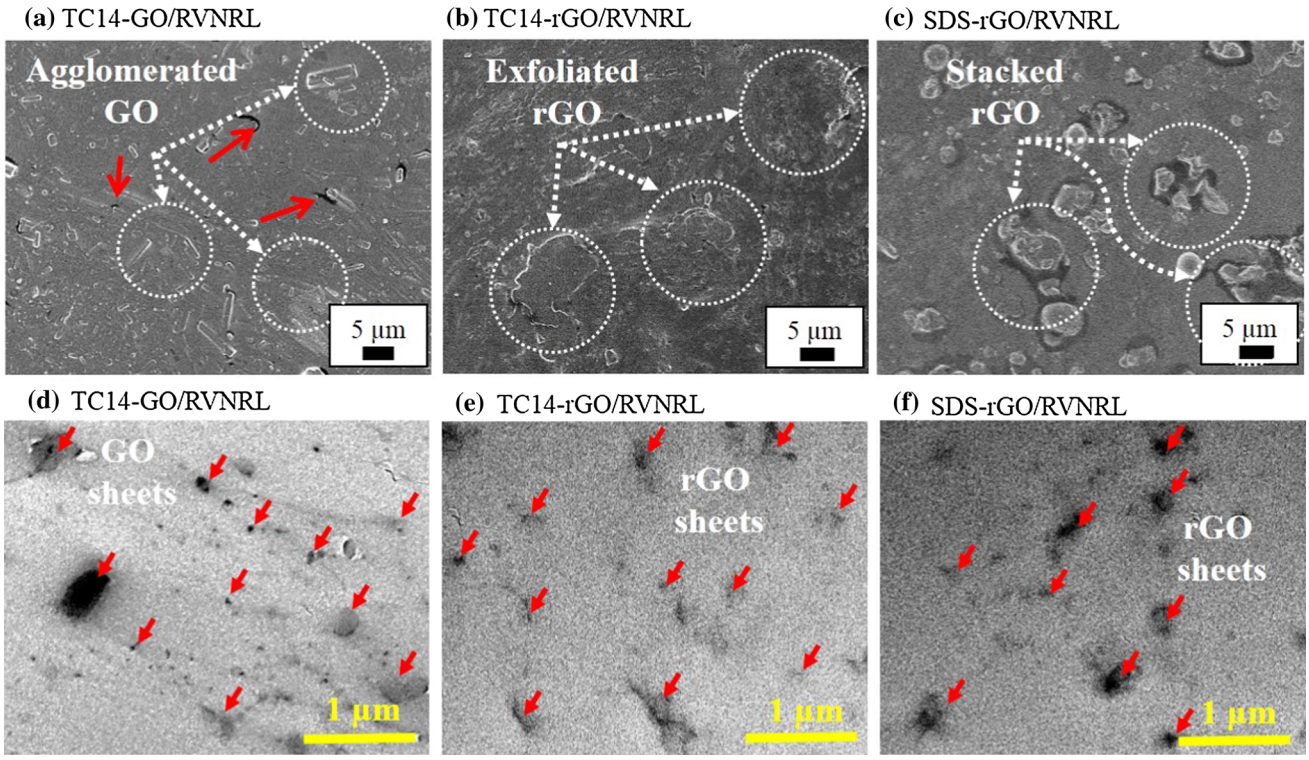

Figure 3 FESEM and HRTEM images of nanocomposite.

rGO dispersions. The measured capacitance is applicable and reliable when considering the electrodes were free from other carbon additives. In comparison, the SDS-rGO/RVNRL polymer nanocomposite shows a low specific capacitance of 11 F g^{-1} (Fig. 1d). This sample presents the lowest capacitive performance among all nanocomposites embedded with GO-assisted TC14. This result is consistent with electrical conductivity measurements, where the used of low surface tension of tripletails of TC14 at higher than the cmc in the RVNRL matrix induced effective adsorption onto the rGO sheets. Therefore, large surface sheets were obtained and a pathway for ion transfer between the electrolyte and electrode was easily formed.

Pristine GO- and rGO-assisted surfactants were further characterized by HRTEM (Fig. 2a–c). The typical wavy appearances of multilayer GO sheets due to the oxidation process were observed (Fig. 2a). Meanwhile, Fig. 2b shows the highly crumpled and large transparent sheets of rGO resulting from the chemical reduction process. However, the absence of transparent characteristics of rGO assisted by SDS was probably due to the stacking of multiple sheets (Fig. 2c). The successful reduction process was also shown by the shifted peak of 227 nm in GO to the higher wavelength of 253 nm (rGO) (Fig. 2d), which was due to the restoring π–π conjugation within the graphitic structures. This was attributed to the conversion of functional groups through the reduction process [23].

Upon incorporation of GO and rGO into the RVNRL matrix, the FESEM image of fractured and few cracked surfaces was observed in the TC14-GO/RVNRL nanocomposite (arrows in Fig. 3a). These characteristics confirmed the interaction of linked–radiated chain with the GO surfaces [40]. Meanwhile, the TC14-rGO/RVNRL nanocomposite shows better distribution of rGO sheets with a few aggregations (shows by circles in Fig. 3b). This was due to the low affinity between the TC14-rGO sheets and the RVNRL matrix which were attributed to successful reduction process of rGO [41]. In comparison, the rGO/RVNRL nanocomposite assisted by SDS surfactant showed highly agglomerated rGO sheets which consequence from the low effective interaction between the SDS-rGO dispersions and the RVNRL matrix (Fig. 3c). HRTEM images of the GO/RVNRL nanocomposite assisted by TC14 surfactant (Fig. 3d) also show obvious unexfoliated sheets as compared with rGO/RVNRL nanocomposite where a uniform

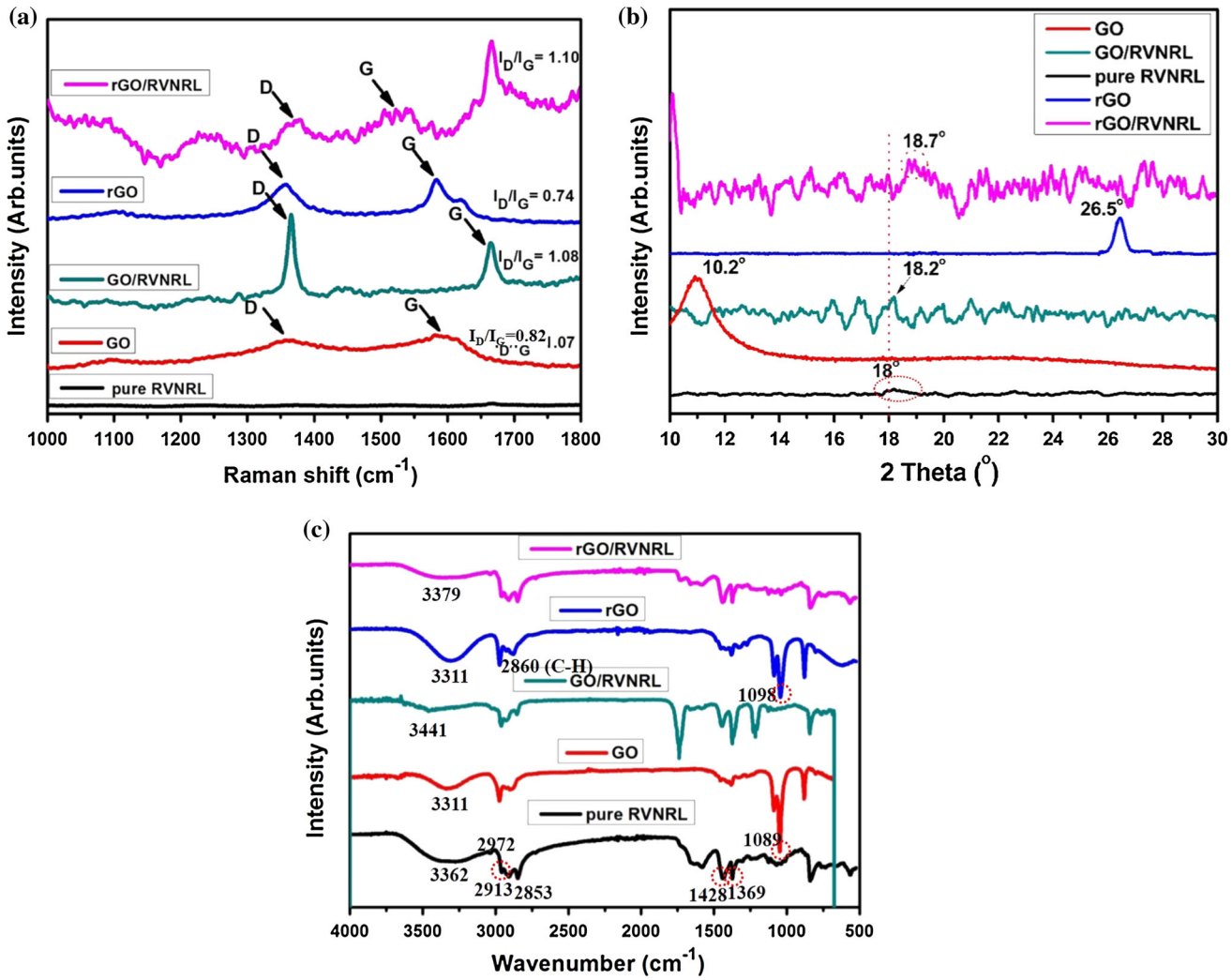

Figure 4 Micro-Raman, XRD, and FT-IR analysis of pristine GO, rGO, and nanocomposite.

and well-dispersed nanocomposite was detected (Fig. 3e). In comparison with the nanocomposite assisted by SDS surfactant, a largely significant size of agglomerated rGO sheet was observed (Fig. 3f) which led to the lowest conductivity nanocomposite films.

Micro-Raman analysis was used to further evaluate the dispersion level and the crystallinity of the samples, as shown in Fig. 4a. The intensity of D to G band for the pristine GO (0.82) was slightly higher than that of pristine rGO, which was found to be 0.74. The decrease in I_D/I_G ratio was due to the defect reduction at the rGO edges caused by the strong reduction that suppressed the oxygen on the surface [42], signifying the rise of sp^2 carbon intensities within the rGO sites [37, 43]. In addition, the result obtained indicated the successful elimination process of the several functional groups from the GO structures using hydrazine hydrate. With the addition of rGO in the RVNRL matrix, the increase in I_D/I_G ratio and slightly higher in the rGO/RVNRL nanocomposite ($I_D/I_G = 1.10$) than the GO/RVNRL nanocomposite (($I_D/I_G = 1.08$) was observed. This result was due to the increase in rGO ripples and the presence of other impurities such as organic dopants through the harsh oxidation–reduction process, which retained the significant defect level in the nanocomposite [44].

The homogeneity of the prepared samples was further confirmed by XRD analysis. Figure 4b shows the pristine GO and rGO, as well as pure RVNRL, GO/RVNRL, and rGO/RVNRL nanocomposites. The broad and low-intensity peak at 18° for pure RVNRL matrix confirmed the amorphous nature. Meanwhile, a shifted peak of GO from ~10.2° to 26.5° was due to

the reduction process [35, 45]. In the nanocomposite sample, the disappearance of the sharp peak at 26.5° corresponding to the unoxidized graphite was observed, indicating that GO and rGO were completely exfoliated in the RVNRL matrix. The rGO/RVNRL nanocomposite showed a broad and high-intensity peak at 18.7° than the GO/RVNRL nanocomposite (18.2°), indicating better distribution of rGO sheets in the RVNRL matrix. This was due to the high surface area obtained from rGO that offered a large space for RVNRL particle to be intercalated and increased the interaction between rGO and RVNRL matrix.

The interfacial interaction was further confirmed using FT-IR analysis. Figure 4c shows the FT-IR spectra of pure RVNRL, pristine GO and rGO, GO/RVNRL, and rGO/RVNRL nanocomposites. For pristine rGO, a clear and broad peak was observed at 2860 cm^{-1} and attributed to C–H bonding. Meanwhile, in the case of pure RVNRL, prominent peaks at 1369, 1428, 2853, 2913, 2972, and 3362 cm^{-1} were observed, which were attributed to the typical NRL functional groups [46]. The shifted peak from 1089 to 1098 cm^{-1} in the rGO spectrum provided evidence for the reduction of GO [47]. The observed hydroxyl band around 3311 cm^{-1} in rGO and GO spectra shifted to a higher wavelength, which was found to be 3379 cm^{-1} for rGO/RVNRL and 3441 cm^{-1} for GO/RVNRL nanocomposite. A low shifted peak at around 68 cm^{-1} for rGO/RVNRL nanocomposite compared with GO/RVNRL nanocomposite (130 cm^{-1}) was correlated to the high interaction of hydrogen bond between rGO dispersion and RVNRL matrix possibly due to reduction [47]. In addition, the remaining oxygen functional groups on the rGO facilitated the physical and chemical interactions between the rGO sheets and RVNRL matrix [48].

TGA analysis is useful for the evaluation of polymer thermal stability. Figure 5a, b shows the thermogravimetric curves of pure RVNRL, pristine GO and rGO, GO/RVNRL, and rGO/RVNRL nanocomposites. Figure 5a shows the enhanced thermal stability of pristine rGO as compared with GO. A gradually decreasing pattern was observed for both curves. The calculated residue weight loss for pristine rGO was found to be ~35%, which was higher than that of pristine GO (~15%). This finding demonstrated the successful elimination of several oxygen functional groups anchored onto the GO structures using hydrazine hydrate [49]. Meanwhile, careful observation showed that the rGO/RVNRL nanocomposite presents a high thermal stability at the onset decomposition temperature of 276 °C as compared with GO/RVNRL nanocomposite (196 °C) and its pure form, RVNRL (~100–250 °C) (Fig. 5b). This result indicated that the addition of rGO in the nanocomposite caused a shifted curve to higher temperature, which was probably due to a sheet barrier effect that reduced the volatilization activity of RVNRL and to the higher heat capacity of rGO itself as compared with the RVNRL matrix [50, 51]. This finding has also been reported by Rajkumar

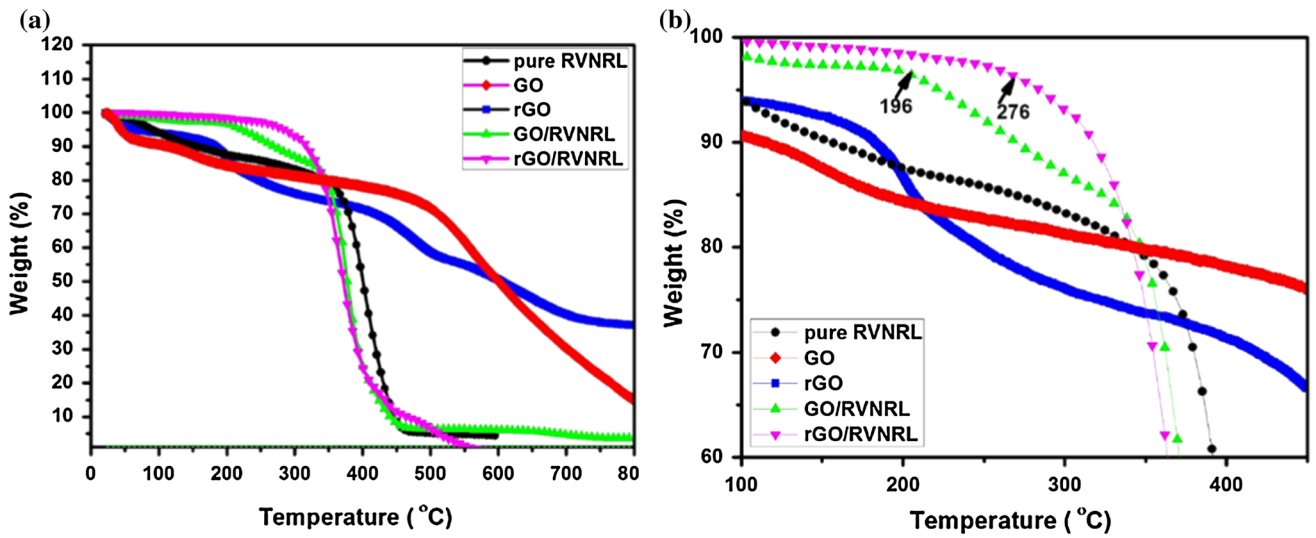

Figure 5 TGA analyses of pristine GO, rGO, and nanocomposite.

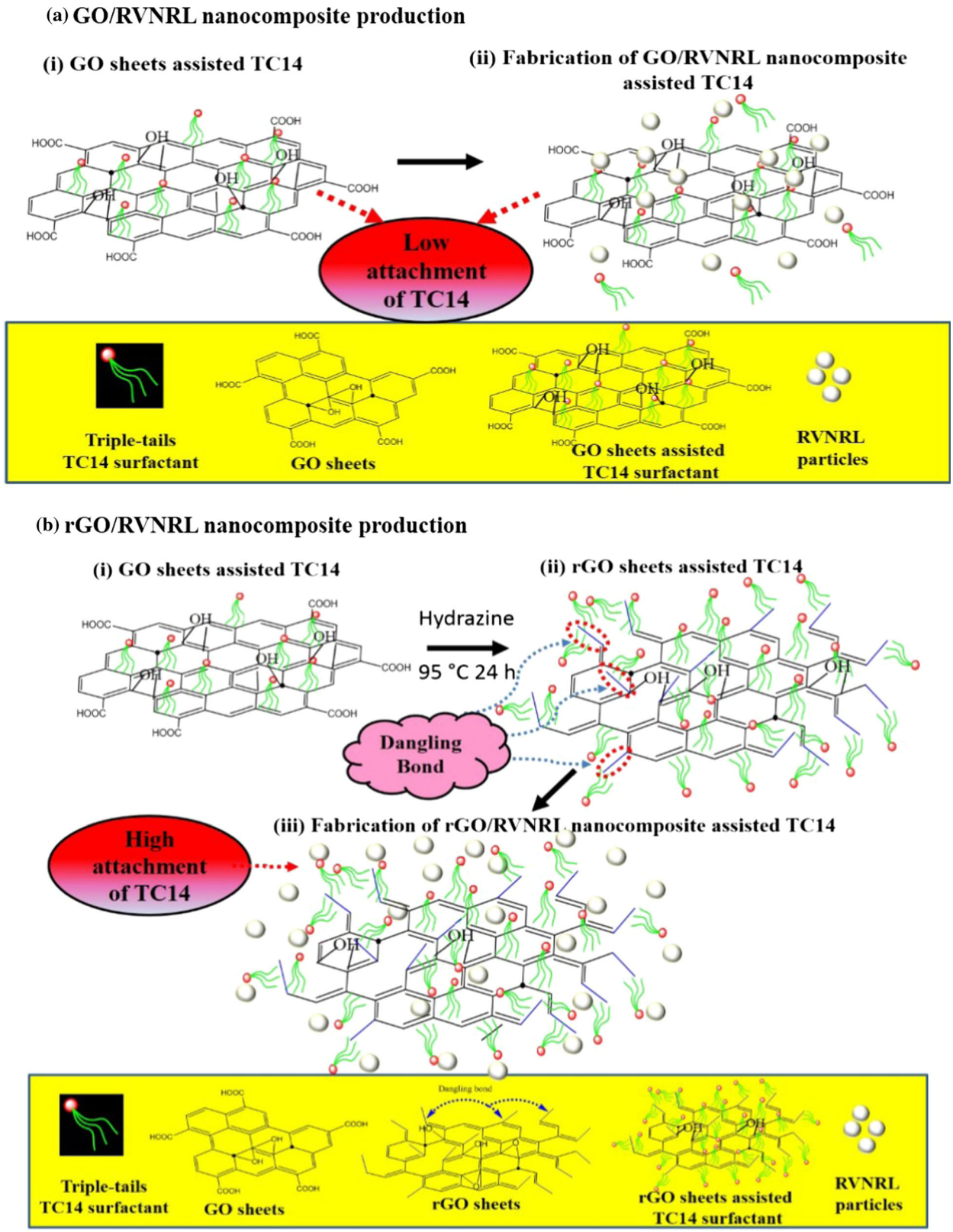

Figure 6 Proposed mechanism of nanocomposite.

et al. [52], where a high thermal stability of nanocomposite was achieved by adding nanographite to a rubber matrix.

The proposed mechanism of the electrical conductivity enhancement of the nanocomposite is shown in Fig. 6a–b. A typical synthesized GO was usually loaded with an abundance of oxygen functional groups at the basal plane and the edges structure [30, 33, 53]. The GO surface with the oxygeneous groups hindered the low surface tension TC14 to have free access along the GO surface, and this led to a minimum number of the attachment TC14 on the GO structure [Fig. 6a(i)]. This may result in a slightly low homogeneity and electrical conductivity obtained for GO when composited in the RVNRL matrix [Fig. 6a(ii)]. Meanwhile, upon the reduction process, the epoxide and carboxylate groups were successfully eliminated with a small quantity of the hydroxyl groups [53] [Fig. 6b(i–ii)]. This then promoted reactive and radical sites of rGO structure, which subsequently formed dangling bonds. This offered an advantage to the existing electron clouds at tailgroup TC14 in the system to attach onto the dangling bond spaces. The highly reactive sites of rGO increased the numbers of the attached tail groups onto the rGO surfaces and thus increased the conductive pathways [30–32, 54] [Fig. 6b(ii)]. In addition, the use of RVNRL polymer containing an alkyl radicals was promoted to a new hydrogen bond formation between the TC14-rGO sheets and the RVNRL matrix [40] [Fig. 6b(iii)]. The increase in interactions and highly accessible tailgroup TC14 surfactant onto the rGO sheets after the reduction process paved a new pathway for the electron transport of free radicals within the TC14-rGO/RVNRL nanocomposite, as supported by the I–V and C–V analyses.

Conclusion

The rGO/RVNRL nanocomposite assisted by TC14 performed the highest electrical conductivity and capacitive value of $\sim\times10^{-3}$ S cm^{-1} and 95 F g^{-1}, respectively, as compared with GO/RVNRL ($\sim\times10^{-4}$ S cm^{-1} and 63 F g^{-1}). The electrical conductivity obtained was two orders of magnitude higher than that of rGO/RVNRL nanocomposite assisted by SDS ($\sim\times10^{-5}$ S cm^{-1}). The possible reasons were the increased number of attached tripletail TC14 on the reactive site of rGO dangling bonds after reduction. The existence of alkyl free radicals in RVNRL matrix also promoted a new hydrogen bond formation and increased the interaction between the rGO and the RVNRL matrix. This phenomenon resulted in higher electrical conductivity and capacitive value, as well as improved uniformity of nanocomposite produced. Thus, a conductive TC14-rGO/RVNRL nanocomposite paved the way for cost-effective, highly bendable electrodes with potential application in fast charge–discharge supercapacitors.

Acknowledgements

The authors would like to express their appreciation to the National Nanotechnology Directorate Division (2014-0015-102-03) and Fundamental Research Grant Scheme (Grant Code: 2015-0154-102-02) for their financial support.

References

[1] Salimi D, Khorasani SN, Abadchi MR, Veshare SJ (2009) Optimization of physic-mechanical properties of silicate-filled NR/SBR compounds. Adv Polym Technol 28(4): 224–232

[2] Rajan VV, Dierkes WK, Joseph R, Noordermeer JWM (2006) Science and technology of rubber reclamation with special attention to NR-based waste latex products. Prog Polym Sci 31(9):811–834

[3] Lopez Manchado MA, Herrero B, Aroro M (2003) Preparation and characterization of organoclay nanocomposites based on natural rubber. Polym Int 52(7):1070–1077

[4] Atieh MA, Nazir N, Yusof F, Fettouhi M, Ratnam CT, Alharthi M, Abu Ilaiwi FA, Mohammed K, Amer AA (2010) Radiation vulcanization of natural rubber latex loaded with carbon nanotubes. Fuller. Nanotub. Carb. Nanostruct. 18(1):56–71

[5] Shen X-J, Pei X-Q, Fu S-Y, Friedrich K (2013) Significantly modified tribological performance of epoxy nanocomposites at very low graphene oxide content. Polymer 54(3): 1234–1242

[6] Stephen R, Jose S, Joseph K, Thomas S, Oommen Z (2006) Thermal stability and ageing properties of sulphur and gamma radiation vulcanized natural rubber (NR) and carboxylated styrene butadiene rubber (XSBR) lattices and their blends. Polym Degrad Stab 91(8):717–1725

[7] Kemp I (1959) Improvements in the vulcanisation of aqueous dispersions of rubber. Br Pat 816:230–242

[8] Hernàndez M, del Mar Bernal M, Verdejo R, Ezquerra TA, Lapez-Manchado MA (2012) Overall performance of natural rubber/graphene nanocomposites Compos. Sci Technol 73:40–46

[9] Gong L-X, Zhao L, Tang L-C, Liu H-Y, Mai Y-W (2015) Balanced electrical, thermal and mechanical properties of epoxy composites filled with chemically reduced graphene oxide and rubber nanoparticles. Compos Sci Technol 121:104–114

[10] George N, Chandra J, Mathiazhagan A, Joseph R (2015) High performance natural rubber composites with conductive segregated network of multiwalled carbon nanotubes. Compos Sci Technol 116:33–40

[11] Li P, Zheng Y, Li M, Shi T, Li D, Zhang A (2016) Enhanced toughness and glass transition temperature of epoxy nanocomposites filled with solvent-free liquid-like nanocrystal-functionalized graphene oxide. Mater Des 89:653–659

[12] Alexandre M, Dubois P (2000) Polymer-layered silicate nanocomposites: preparation, properties and uses of a new class of materials. Mater Sci Eng R Rep 28(1):1–63

[13] Jana SC, Jain S (2001) Dispersion of nanofillers in high performance polymers using reactive solvents as processing aids. Polymer 42(16):6897–6905

[14] Favier V, Cavaille JY, Canova GR, Shrivastava SC (1997) Mechanical percolation in cellulose whisker nanocomposites. Polym Eng Sci 37(10):1732–1739

[15] Chiu F-C (2016) Fabrication and characterization of biodegradable poly(butylene succinate-co-adipate) nanocomposites with halloysite nanotube and organo-montmorillonite as nanofillers. Polym Test 54:1–11

[16] Shokrieh MM, Esmkhani M, Haghighatkhah AR, Zhao Z (2014) Flexural fatigue behaviour of synthesized graphene/carbon-nanofiber/epoxy hybrid nanocomposites. Mater Des 62:401–408

[17] Yan Q, Liu Q, Wang J (2016) A simple and fast microwave assisted approach for the reduction of graphene oxide. Ceram Int 42(2):3007–3013

[18] Hu K, Kulkarni DD, Choi I, Tsukruk VV (2014) Graphene-polymer nanocomposites for structural and functional applications. Prog Polym Sci 39(11):1934–1972

[19] Kang XJ, Zhang JM, Sun XW, Zhang FR, Zhang YX (2016) One-pot synthesis of vanadium dioxide nanoflowers on graphene oxide. Ceram Int 42(6):7883–7887

[20] Min C, Yu D, Cao J, Wang G, Feng L (2013) A graphite nanoplatelet/epoxy composite with high dielectric constant and high thermal conductivity. Carbon 55:16–125

[21] Zhu P, Shen M, Xiao S, Zhang D (2011) Experimental study on the reducibility of graphene oxide by hydrazine hydrate. Phys B 406(3):498–502

[22] She X, Zhang X, Liu J, Li L, Yu Z, Huang Z, Shang S (2015) Microwave-assisted synthesis of Mn_3O_4 nanoparticles@ reduced graphene oxide nanocomposites for high performance supercapacitors. Mater Res Bull 70:945–950

[23] Marlinda AR, Huang NM, Muhamad MR, An'Amt MN, Chang BYS, Yusoff N, Harrison L, Lim HN, Chia CH, Kumar SV (2012) Highly efficient preparation of ZnO nanorods decorated reduced graphene oxide nanocomposites. Mater. Lett. 80:9–12

[24] Agharkar M, Kochrekar S, Hidouri S, Azeez MA (2014) Trends in green reduction of graphene oxides, issues and challenges: a review. Mater Res Bull 59:323–328

[25] Jin Y, Huang S, Zhang M, Jia M, Hu D (2013) A green and efficient method to produce graphene for electrochemical capacitors from graphene oxide using sodium carbonate as a reducing agent. Appl Surf Sci 268:541–546

[26] Åšliwak A, Grzyb B, Daez N, Gryglewicz G (2016) Nitrogen-doped reduced graphene oxide as electrode material for high rate supercapacitors. Appl Surf Sci 399:265–271. doi:10.1016/j.apsusc.2016.12.060

[27] El Achaby M, Qaiss A (2013) Processing and properties of polyethylene reinforced by graphene nanosheets and carbon nanotubes. Mater Des 44:81–89

[28] Malas A, Pal P, Das CK (2014) Effect of expanded graphite and modified graphite flakes on the physical and thermo-mechanical properties of styrene butadiene rubber/polybutadiene rubber (SBR/BR) blends. Mater Des 55:664–673

[29] Li Y, Pan D, Chen S, Wang Q, Pan G, Wang T (2013) In-situ polymerization and mechanical, thermal properties of polyurethane/graphene oxide/epoxy nanocomposites. Mater Des 47:850–856

[30] Suriani AB, Nurhafizah MD, Mohamed A, Masrom AK, Sahajwalla V, Joshi RK (2016) Highly conductive electrodes of graphene oxide/natural rubber latex-based electrodes by using a hyper-branched surfactant. Mater Des 99:174–181

[31] Mohamed A, Anas AK, Suriani AB, Aziz AA, Sagisaka M, Brown P, Eastoe J, Kamari A, Hashim N, Isa IM (2014) Preparation of multiwall carbon nanotubes (MWCNTs) stabilised by highly branched hydrocarbon surfactants and dispersed in natural rubber latex nanocomposites. Colloid Polym Sci 292(11):3013–3023

[32] Mohamed A, Anas AK, Suriani AB, Ardyani T, Zin WMW, Ibrahim S, Sagisaka M, Brown P, Eastoe J (2015) Enhanced dispersion of multiwall carbon nanotubes in natural rubber latex nanocomposites by surfactants bearing phenyl groups. Colloid Interface Sci 455:179–187

[33] Suriani AB, Nurhafizah MD, Mohamed A, Zainol I, Masrom AK (2015) A facile one-step method for graphene oxide/natural rubber latex nanocomposite production for supercapacitor applications. Mater Lett 161:665–668

[34] Mohamed A, Ardyani T, Suriani AB, Brown P, Hollamby M, Sagisaka M, Eastoe J (2016) Graphene-philic surfactants for nanocomposites in latex technology. Adv Colloid Interface Sci 230:54–69

[35] Fouda AN, Assy MKA, El Enany G, Yousf N (2015) Enhanced capacitance of thermally reduced hexagonal graphene oxide for high performance supercapacitor. Fuller Nanotub Carb Nanostruct 23(7):618–622

[36] Oraon R, De Adhikari A, Tiwari SK, Sahu TS, Nayak GC (2015) Fabrication of nanoclay based graphene/polypyrrole nanocomposite: an efficient ternary electrode material for high performance supercapacitors. Appl Clay Sci 118:231–238

[37] Wang G, Wang B, Park J, Wang Y, Sun B, Yao J (2009) Highly efficient and large-scale synthesis of graphene by electrolytic exfoliation. Carbon 47(14):3242–3246

[38] Li X, Zhang G, Bai X, Sun X, Wang X, Wang E, Dai H (2008) Highly conducting graphene sheets and Langmuir–Blodgett films. Nat Nanotechnol 3(9):538–542

[39] Wang S, Ma L, Gan M, Fu S, Dai W, Zhou T, Sun X, Wang H, Wang H (2015) Free-standing 3D graphene/polyaniline composite film electrodes for high-performance supercapacitors. J Power Sourc 299:347–355

[40] Makuuchi K (2003) An introduction to radiation vulcanization of natural rubber latex. TRI Global Co., Bangkok

[41] Liu X, Kuang W, Guo B (2015) Preparation of rubber/graphene oxide composites with in situ interfacial desirable. Polymer 56:553–562

[42] Guardia L, Paredes JI, Fernandez-Merino MJ, Solis-Fernandez P, Villar-Rodil S, Martinez-Alonso A, Tascan JMD (2011) High-throughput production of pristine graphene in an aqueous dispersion assisted by non-ionic surfactants. Carbon 49:1653–1662

[43] Yaragalla S, Meera AP, Kalarikkal N, Thomas S (2015) Chemistry associated with natural rubber-graphene nanocomposites and its effect on physical and structural properties. Ind Crops Prod 74:792–802

[44] Ryu SH, Shanmugharaj AM (2014) Influence of long-chain alkylamine-modified graphene oxide on the crystallization, mechanical and electrical properties of isotactic polypropylene nanocomposite. Chem Eng 244:552–560

[45] Ashori A, Rahmani H, Bahrami R (2015) Preparation and characterization of functionalized graphene oxide/carbon fiber/epoxy nanocomposites. Polym Test 48:82–88

[46] Pichayakorn W, Suksaeree J, Boonme P, Taweepreda W, Ritthidej GC (2012) Preparation of deproteinized natural rubber latex and properties of films formed by itself and several adhesive polymer blends. Ind Eng Chem Res 51(41):13393–13404

[47] Li X, Umar A, Chen Z, Tian T, Wang S, Wang Y (2015) Supramolecular fabrication of polyelectrolyte-modified reduced graphene oxide for NO_2 sensing applications. Ceram Int 41(9):12130–12136

[48] Chen G, Weng W, Wu D, Wu C (2003) PMMA/graphite nanosheets composite and its conducting properties. Eur Polym 39(12):2329–2335

[49] Wang X, Yang H, Song L, Hu Y, Xing W, Lu H (2011) Morphology, mechanical and thermal properties of graphene-reinforced poly(butylene succinate) nanocomposites. Compos Sci Technol 72(1):1–6

[50] Teng C-C, Ma C-CM, Lu C-H, Yang S-Y, Lee S-H, Hsiao M-C, Yen M-Y, Chiou K-C, Lee T-M (2011) Thermal conductivity and structure of non-covalent functionalization graphene/epoxy composites. Carbon 49(15):5107–5116

[51] Malas A, Das CK, Das A, Heinrich G (2012) Development of expanded graphite filled natural rubber vulcanizates in presence and absence of carbon black: mechanical, thermal and morphological properties. Mater Des 39:410–417

[52] Rajkumar K, Kumari N, Ranjith P, Chakraborty SK, Thavamani P (2011) High temperature resistance properties of NBR based polymer nanocomposites. Int J ChemTech Res 3(3):1343–1348

[53] Ren P-G, Yan D-X, Ji X, Chen T, Li Z-M (2010) Temperature dependence of graphene oxide reduced by hydrazine hydrate. Nanotechnology 22(5):055705. doi:10.1088/0957-4484/22/5/055705

[54] Yan L, Zheng YB, Zhao F, Li S, Gao X, Xu B, Weiss PS, Zhao Y (2012) Chemistry and physics of a single atomic layer: strategic and challenges for functionalization of graphene and graphene-based materials. RSC 41(1):97–114